ENGINEERING JOURNAL

Article

The Monitoring of H_2S and SO_2 Noxious Gases from Industrial Environment with Sensors Based on Flame-spray-made SnO_2 Nanoparticles

Chaikarn Liewhiran[1,4,*], Nittaya Tamaekong[2], Anurat Wisitsora-at[3], and Sukon Phanichphant[4]

1 Department of Physics and Materials Science, Faculty of Science, Chiang Mai University, Chiang Mai 50200, Thailand
2 Program in Materials Science, Faculty of Science, Maejo University, Chiang Mai 50290, Thailand
3 Nanoelectronics and MEMS Laboratory, National Electronics and Computer Technology Center, Klong Luang, Pathumthani 12120, Thailand
4 Materials Science Research Center, Faculty of Science, Chiang Mai University, Chiang Mai 50202, Thailand
E-mail: chaikarn_l@yahoo.com*

Abstract. The noxious gas sensors were developed successfully using flame-spray-made SnO_2 nanoparticles as the sensing materials. The functionalized nanoparticle properties were further analyzed by XRD, BET and TEM analyses. The SnO_2 nanoparticles (SSA_{BET}: 141.6 m^2/g) were investigated revealing non-agglomerated spherical, hexagonal, rectangle (3–10 nm), and rod-like (3–5 nm in width and 5–20 nm in length) morphologies. The sensing films were prepared by spin coating onto the Al_2O_3 substrates interdigitated with Au electrodes. The sensing films were significantly developed in order to detect with H_2S (0.5–10 ppm) and SO_2 (20–500 ppm) at the operating temperature ranging from 200-350°C. After sensing test, the cross-section of sensing film was analyzed by SEM analyses. It was found that SnO_2 sensing film showed higher sensitivity to H_2S gas with very fast response at lower concentrations (3s, to 10 ppm). The cross sensitivities of the sensor towards different concentrations of H_2S, CO, H_2, and C_2H_2 were measured at 300°C. The sensor evidently shows much less response to CO, H_2, and C_2H_2 than to H_2S indicating higher selectivity for H_2S of the SnO_2 sensor at the lower concentration (10 ppm). Therefore, the SnO_2 sensor was the most suitable candidate for the efficient detection of H_2S noxious gas.

Keywords: H_2S, SO_2, noxious gas, environmental sensors, SnO_2, flame spray pyrolysis.

ENGINEERING JOURNAL Volume 16 Issue 3
Received 18 November 2011
Accepted 6 February 2012
Published 1 July 2012
Online at http://www.engj.org/
DOI:10.4186/ej.2012.16.3.123

This paper is based on the oral presentation at the German-Thai Symposium on Nanoscience and Nanotechnology 2011—Green Nanotechnology of the Future, GTSNN 2011, in Nakhon Ratchasima, Thailand, 13-16 September 2011.

DOI:10.4186/ej.2012.16.3.123

1. Introduction

Hydrogen sulfide (H_2S) is a toxic gas produced from the coal, oil, and natural gas industries [1–7]. The high toxicity of H_2S, which has significant negative impacts on health and the environment, has attracted attention to monitor and control this gas. With a maximum allowed limit in the atmosphere of 10 ppm H_2S [6], developing reliable sensors with high sensitivity and also selectivity towards other gases is a real challenge. Sulfur dioxide (SO_2) gas is one of the most toxic and common air pollutants [4, 8, 9]. Due to growing concern on environmental issues, much attention has been focused on the monitoring of air pollutants. SO_2 is one of the major gases that cause a serious air pollution problem. The most important application falls in the category where human beings cannot afford to risk smelling noxious gases. Also, an exposure to SO_2 can cause irritation to eyes, skin and respiratory system. These are the reason for increasing requirements to monitor the gas pollutions in urban agglomerates or in the work ambient atmosphere [8, 9]. The long-term exposure limit and the short-term exposure limit of sulfur dioxide gas are 2–5 ppm, respectively, although the acceptable limit of SO_2 in ambient air is much less. Nevertheless, the monitoring of SO_2 leakage at the source may be helpful to contain not only the accidental exposure at the source but also environmental pollution in general [8, 9]. Therefore, rapid detections of poisonous and hazardous gases including H_2S and SO_2 in technological wastes are challenging.

Recently, metal oxide semiconductors (MOS) [10–17] have been extensively investigated for this purpose due to their simplicity, small dimensions and attractive price. Several types of metal oxide semiconductors have been used as sensing material for different type of gases. SnO_2 is one of the most promising materials for sensor and has attractively established the attention of many users and scientists' interest in gas sensing under atmospheric conditions. It is a wide band gap and the best-understood prototype of oxide-based gas sensors for the detection of various noxious gases especially H_2S and SO_2 [1–9]. In the present study, Flame Spray Pyrolysis (FSP) is presented as a very promising technique for sensor material fabrication since it enables primary particle and crystal size control [18, 19], which is important to improve the sensitivity, as well as controlling in situ deposition of noble metal clusters [19]. It has been shown that due to the morphology of the FSP-made particles, the mass transfer rates in catalysis are higher compared to microporous material because of the large external surface area of flame-made materials [19, 20]. Moreover, the importance of the size control, the required large and easily accessible surface area (large pore size, no micropores), the efficiency of noble metal doping, and competitive production rates put high demands on the method of nanoparticles production for sensor materials. Therefore, it is interesting to apply FSP for production of SnO_2 nanoparticles to be used in environmental gas sensors. In this work, the applicability of FSP in synthesis of SnO_2 nanoparticles for noxious gas sensing from industrial environment is reported. The aim is to demonstrate that the FSP process in general can be successfully applied for sensor material production and to specifically evaluate the noxious i.e. H_2S and SO_2 performance of environmental gas sensors.

2. Experimental

2.1. Flame Synthesis

Figure 1 shows the set up for FSP process used to produce the flame-spray-made SnO_2 nanopowders. Precursor solutions (0.50 M) were prepared by dissolving appropriate amounts of tin (II) 2-ethylhexanoate (Aldrich, 95%) used as Sn in xylene (Carlo Erba, 98.5%). The precursor mixture was fed into a nozzle at a constant feed rate of 5 ml/min using a syringe pump. At the end of the nozzle the precursor solution was dispersed by 4.30 l/min oxygen forming a spray with a pressure drop at the capillary tip kept constant at 1.5 bars by adjusting the orifice gap area. A sheath gas flow of 3.92 l/min of O_2 was supplied concentrically around the nozzle to stabilize and control the spray flame. The spray was ignited by supporting flamelets fed with oxygen (2.46 l/min) and methane (1.19 l/min), which were positioned in a ring around the nozzle outlet. The observed flame height was approximately 10 cm and appearance was light orange. The combustion enthalpies were directly dependent on the particular solvent, starting materials. After evaporation and combustion of precursor droplets, particles were formed by nucleation, condensation, coagulation, and coalescence. Finally, the nanopowders were collected on a glass microfibre filters (Whatmann GF/A, 25.7 cm in diameter) with the aid of a vacuum pump (Busch, Seco SV 1040C).

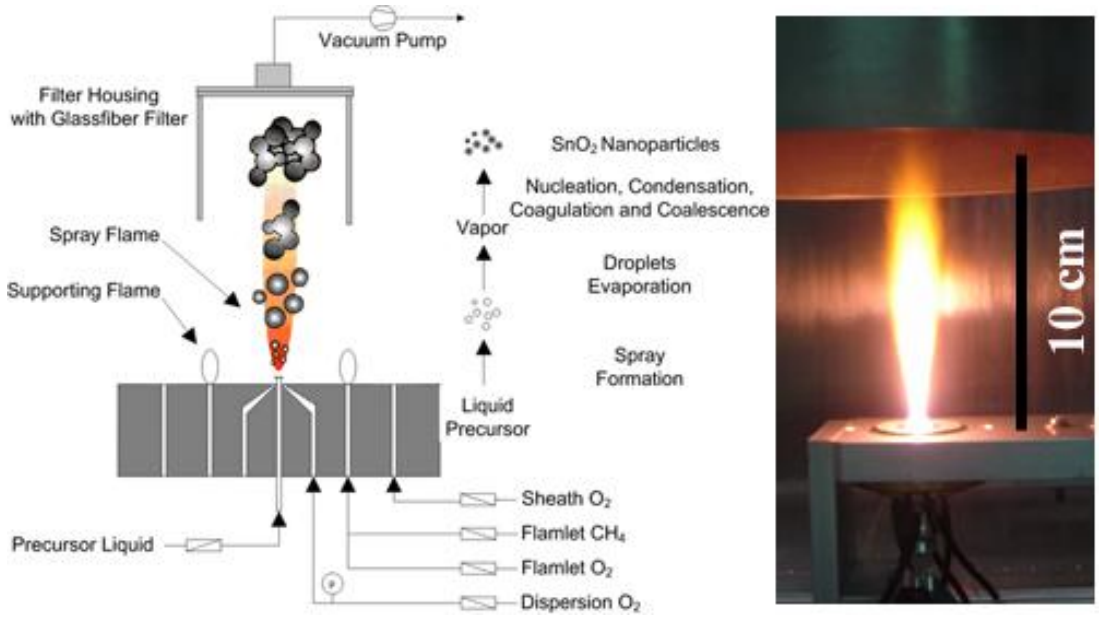

Fig. 1. Schematic diagram of FSP process and flame appearance.

2.2. Nanopowder Characterizations

The nanopowders phase was analyzed by X-ray diffraction (XRD) [Phillips X-'pert] using CuKα radiation (20 kV, 20 mA) with a scanning speed of 5º/min. The Brunauer-Emmett-Teller (BET) specific surface area (SSA_{BET}), was measured by nitrogen adsorption at 78 K [Autosorb 1 MP, Quantachrome] after degassing at 120°C for 2h prior to analysis in nitrogen. Assuming uniform spherical particles within an aggregate, the average equivalent diameter of the primary particles was calculated from $d_{BET} = 6/SSA_{BET} \times \rho_{sample}$, where SSA_{BET} was the specific surface area (m^2/g) and $\rho_{samples}$ was the average density of SnO_2 (ρ_{SnO_2} = 6.85 g/cm^3 [10]). The accurate morphologies of the SnO_2 nanoparticles were determined by transmission electron microscopy (TEM) [JSM-2010, JEOL]. After sensing test, the cross-sectional structures of sensor were observed by scanning electron microscopy (SEM) [JSM-6335F, JEOL] analyses.

2.3. Sensor Preparation

An appropriate quantity of 0.28 mL homogeneous mixed solution was prepared by stirring and heating at 80°C for 12h with ethyl cellulose (Fluka, 30–70 mPa.s) as the temporary binder and terpineol (Aldrich, 90%) as a solvent. The liquid mixture was combined with 60 mg samples of the flame-made SnO_2 nanopowders and mixed for 30 min to form a paste prior to spin-coating. The resulting paste was firstly spin-coated at 700 rpm for 10 s, and then subsequently at 3,000 rpm for 30 s on the Al_2O_3 substrates (0.4 × 0.5 × 0.1 cm) interdigitated with Au electrodes to deposit sensing films. The resulting substrates were annealed in an oven at 150°C for 1h with an annealing rate of 1°C/min and then subsequently annealed at 400°C for 1h with an annealing rate of 1°C/min for binder removal prior to the sensing test.

2.4. Noxious Gases Sensing Measurements

The gas-sensing characteristics of SnO_2 sensing films were characterized over a high concentration range of SO_2 (20–500 ppm). In contrast, it was tested specifically within a low concentration range of H_2S (0.5–10 ppm). The standard flow through technique was used to test the gas-sensing properties of SnO_2 films. A constant flux of synthetic air of 2 l/min as gas carrier was flowed to mix with desired concentration of pollutants dispersed in synthetic air. All measurements were conducted in a temperature-stabilized sealed chamber at 20°C under controlled humidity. The gas flow rates were precisely manipulated using a computer controlled multi-channel mass flow controller. An external NiCr heater was heated by a regulated DC power supply to different operating temperatures ranging from 200-350°C. The resistances of various sensors were continuously monitored with a computer-controlled system by voltage-amperometric

technique with 10 V DC bias and current measurement through a picoammeter. The sensor was exposed to a gas sample for ~5 minutes for each gas concentration testing and then the air flux was restored for 15 minutes. The sensitivity (S) is defined as the resistance ratio R_a/R_g, where R_a is the resistance in dry air, and R_g is the resistance in the test gas. After sensors fabrication, they had been tested with varied the operating temperatures. Finally, the sensing film morphology were observed using SEM analysis.

3. Results and Discussion

3.1. Particle Properties

Figure 2 shows the XRD patterns of flame-spray-made SnO_2 nanopowders. It can be seen that the nanopowders were highly crystalline and all peaks can be confirmed to be the cassiterite-tetragonal phase of SnO_2 from their excellent matching to the JCPDS file NO. 77–447 [symmetrical group: $P_{42/mnm}$] with lattice constants of a=b=0.4735 nm and c=0.3185 nm. Figure 3 illustrates the TEM bright-field image of flame-spray-made pure SnO_2 nanoparticles. The corresponding electron diffraction pattern is shown in the inset. From the TEM bright-field image, SnO_2 primary nanoparticles are polyhedral, non-agglomerated and well dispersed. In addition, flame-spray-made SnO_2 nanoparticles indicate polyhedral aggregates of primary particles. The morphologies of flame made (5/5) SnO_2 and 0.2–3 wt% Ru/SnO_2 nanoparticles contain mainly spherical particles with diameters ranging from 3–10 nm, and occasionally rectangular, hexagonal (3–10 nm) and rod-like (3–5 nm in width, and 5–20 nm in length) particles. From the measured SSA_{BET} for SnO_2 nanoparticles of 141.6 m^2/g, the average BET-equivalent particle diameter is determined to be 6.2 nm. The particle diameters from BET and TEM analysis are in good agreement (d_{BET} = 6.2 nm, d_{TEM} = 3–10 nm). The small primary-particle size and correspondingly large specific surface area of flame-spray-made SnO_2 nanoparticles are highly preferred properties for gas-sensing.

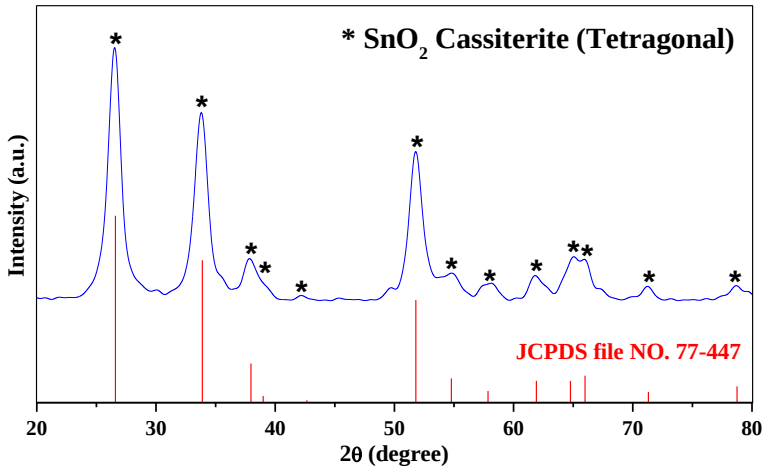

Fig. 2. XRD patterns of flame-spray-made unloaded SnO_2 nanoparticles.

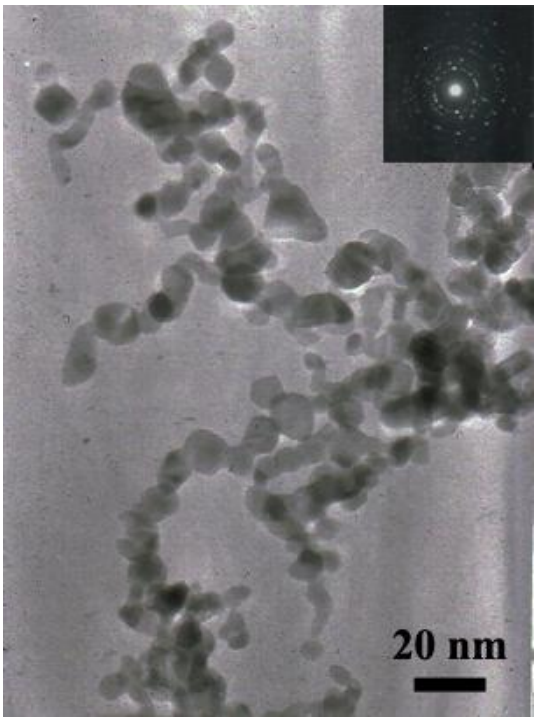

Fig. 3. TEM bright-field image of flame-spray-made unloaded SnO_2 nanoparticles. Non-agglomerated particles can be observed. The corresponding electron diffraction pattern was shown in the inset.

3.2. Noxious Gases (SO_2 and H_2S) Sensing Properties

Figure 4 shows the variation of the sensitivity to H_2S concentration ranging from 0.5–10 ppm with different operating temperatures. It is observed that the sensitivity towards H_2S increases with temperature and attains a maximum value at 300°C, followed by declining with further increase in the operating temperature. It is observed that the SnO_2 sensing films responded to 10 ppm exhibits the highest sensitivity (8.4) to H_2S at 300°C. SnO_2 is an n-type semiconductor in which the adsorbed oxygen reacts with the combustible gas releasing electrons into the conduction band by which the conductivity increases. When the sensors are exposed to air atmosphere, oxygen will be physically and chemically adsorbed on the surface of SnO_2 sensing film. The adsorbed oxygen molecules act as electron acceptors and then form O^{2-}, O_2^-, O^-, generating depleted layers resulting in the release of the large number of free electrons as followed by Eqs. (1–3). The increase of the width and height of the potential barrier at the contacts among nanocrystals and consequently lead to resistance increase of the sensors. Moreover, H_2S is also chemisorbed on the surface and the metal oxide is chemically transformed into sulfides as shown in Eq. (4).

$$H_2S_{(ads)} + 3O_{(s)}^{2-} \rightarrow SO_{2(g)} + H_2O + 6e^- \quad (1)$$

$$2H_2S_{(ads)} + 3O_{2(s)}^{-} \rightarrow 2SO_{2(g)} + 2H_2O + 3e^- \quad (2)$$

$$H_2S_{(ads)} + 3O_{(s)}^{-} \rightarrow SO_{2(g)} + 2H_2O + 3e^- \quad (3)$$

$$2H_2S + SnO_2 \leftrightarrow SnS_2 + 2H_2O \quad (4)$$

DOI:10.4186/ej.2012.16.3.123

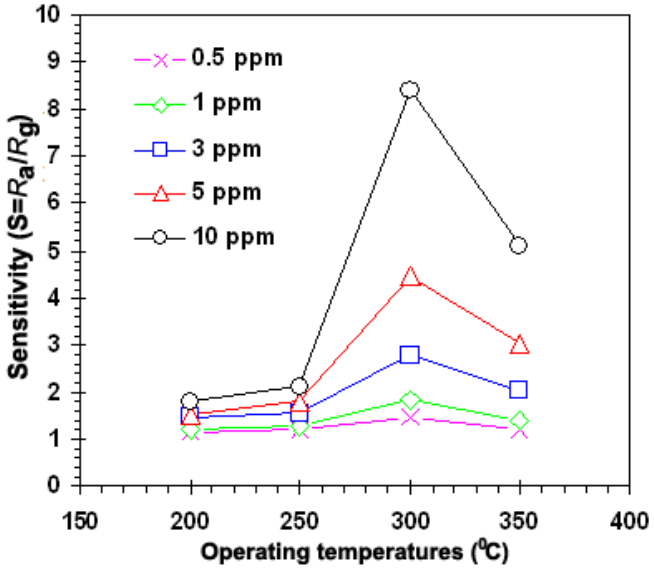

Fig. 4. Variation of the sensitivity to 0.5–10 ppm of H_2S with different the operating temperatures ranging from 200–350°C.

The interaction of the resistive sensors with a target gas produces a change in the electrical conductance of the sensors recorded by a variation in the electrical resistance. Figure 5 shows the change in resistance of SnO_2 sensors under exposure to H_2S pulses with varying concentrations from 0.5 to 10 ppm at operating temperatures ranging from 200–350°C during backward cycle. The resistance reduction is clearly seen at all gas concentrations indicating that the SnO_2 sensor has typical n-type semiconductor behaviors. It can be noticed that the operating temperature at 300°C shows the best response with evident decreasing the resistance than the other operating temperatures. Thus, this suitable operating temperature can greatly improve H_2S response of SnO_2 sensors. In addition, SnO_2 sensor had fast response with rather stable in recovery baseline even at low operating temperature of 300°C.

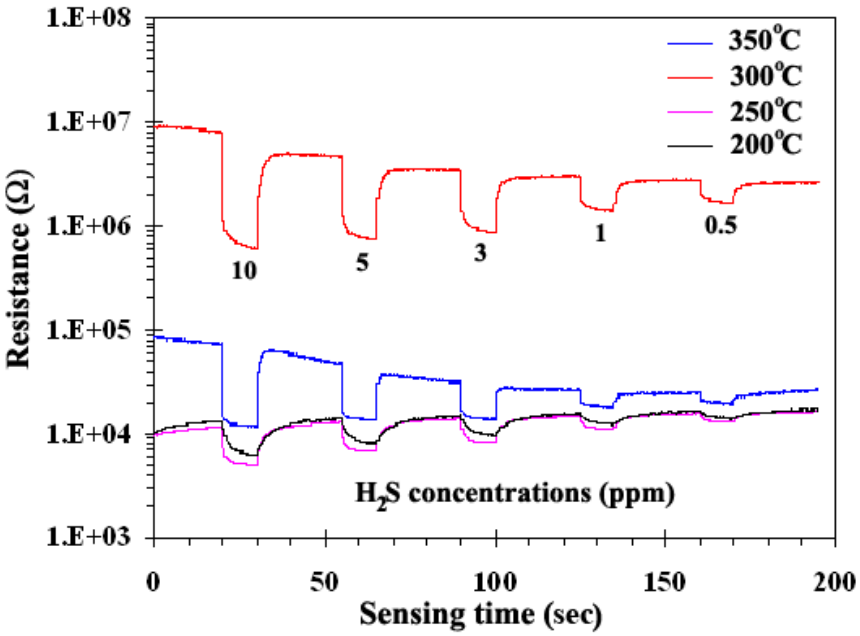

Fig. 5. Change in resistance of SnO_2 sensor upon exposure to H_2S at operating temperatures ranging from 200–350°C.

Figures 6(a) and 6(b) show the plot of response (S) and response times (T_{res}) for the SnO_2 sensor versus concentrations of noxious H_2S (0.5–10 ppm, Fig. 6(a)) and SO_2 (20–500 ppm, Fig. 6(b)) gases at operating temperatures ranging from 200–350°C. In Fig. 6 (a), it was clear that the responses (left) increased and the response times (right) drastically decreased with increasing H_2S concentrations. For both H_2S and SO_2 (Figs. 6 (a) and 6 (b)), it can be seen that sensor had the best sensing performances at 300°C than the other operating temperatures with the highest response and the shortest response times. The better H_2S sensing performance in terms of the response (S=8.4) and response time (3 s) are obtained at the highest concentration (10 ppm) at 300°C, while the response (S=6.9) and response time (12 s) to higher concentration of 500 ppm were considerably lower (Fig. 6 (b)) through performed higher concentration. The SnO_2 sensor shows very fast response to H_2S whereas the responses to SO_2 are somewhat sluggish. While the sensor reveals quite low SO_2response at 500 ppm, H_2S sensing yields much higher response at lower concentration, enabling more accurate detection of the small leakage in an atmosphere form the industrial environment. The superior sensitivity toward H_2Smay be explained from the reaction kinetic of H_2S and SO_2 according to the reaction paths (1) and (5):

$$SO_{2(ads)} + O^{2-}_{(s)} \rightarrow SO_{3(g)} + 2e^{-} \tag{5}$$

It can be seen that H_2S molecule can produce three times of the number of free electrons per reaction compared to that of SO_2 one therefore the sensitivity of the sensor to H_2S is significantly higher. It should also be noted that SO_2 was characterized only in the range of 20–500 ppm because of the limitation of the present gas mixing system, in which the dilution is limited to 2 % of the SO_2 gas source concentration of 2,000 ppm. However, it can be predicted from the gas sensitivity curve (Fig. 6 (b)) that the sensor does not possess appreciable sensitivity toward the exposure limit of 2–5 ppm. Thus, the sensor is not particularly suitable for SO_2 detection in atmosphere.

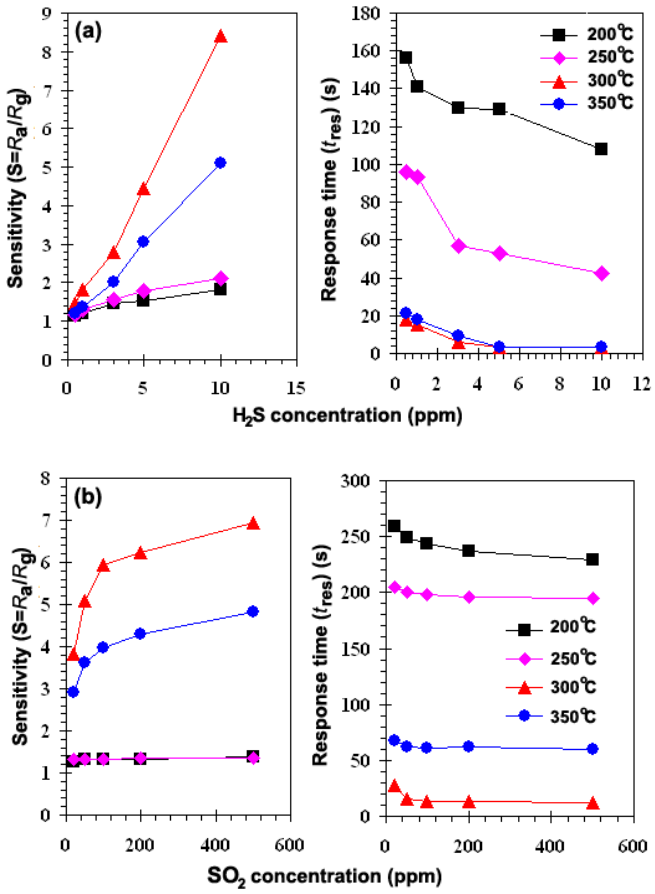

Fig. 6. Sensitivity (left) and corresponding response time (right) of SnO_2 sensors as a function of (a) H_2S and (b) SO_2 concentrations in dry air at the operating ranging from 200–350°C.

The recovery times for these gases (not shown) were within a few minutes. This is due possibly to slow desorption of gas species from highly porous SnO_2 nanostructures. This is consistent with Griessler *et. al* [5] mentioned the nanosensors based on ultrathin SnO_2 films, which were very sensitive to the highly toxic gases SO_2 and H_2S. The SnO_2-sensing films are fabricated by a spray pyrolysis process on Si substrates with a thickness of 50 nm. The sensor resistance was decreased in the presence of the toxic gases. Exposure to 50 ppm SO_2 leads to a sensor resistance drop of ~40% whereas a H_2S gas concentration of only 2.5 ppm decreases the resistance by ~85%, which demonstrates the extraordinary sensitivity of the nanosensors. Furthermore, Ghimbeu *et al.* [7] reported the ability of electrostatic sprayed SnO_2 and CuO/SnO_2 (1, 2, and 4 at.% Cu) films to detect different pollutant gases, i.e., H_2S, SO_2, and NO_2. The SnO_2 films had low response of H_2S (~6 to 10 ppm) and SO_2 (~1 to 20 ppm) at low operating temperature of 100°C. Among the studied films, the 1 at.% Cu-doped SnO_2 layer is the most sensitive in the detection of all the studied gases. Therefore, the SnO_2 sensor has been one of the most suitable candidates for the efficient detection of noxious gases for industrial environment especially H_2S at very low detections limits. The detection limit can be estimated from the characteristic curve using the standard power law for gas sensor. Taking the threshold response for detection limit of 1.05 (resistance change of 5%), the detection limits for H_2S are 0.33, 0.32, 0.35 and 0.49 ppm at 200, 250, 300 and 350°C, respectively. Similarly the detection limits for SO_2 are 5.1, 3.2, 1.0 and 1.9 ppm at 200, 250, 300 and 350°C, respectively. Thus, the sensor has optimal detection limits at 300°C operating temperature for both gases.

A summary of gas-sensing performance of pure SnO_2 prepared by various synthetic methods was shown in Table 1. It can be seen that spin-coated FSP-prepared SnO_2 film in the present work exhibits much better H_2S selectivity than other reported H_2S sensors. The sensor characteristics including response and response/recovery time of sensing films can considerably be affected by the particle morphology, size and distribution as well as operating temperature. The main advantage of FSP includes ability to produce well-controlled nanosized particles with high crystallinity structure suitable for gas sensing. However, the differences between our result and those of other flame-spray-made SnO_2 films suggest that the method for deposition of FSP nanoparticles on substrate is also very important. Spin coating technique used in this work which can produce uniform porous film with high particle density, resulting in relatively larger specific surface area and higher gas adsorption.

3.3. Environmental Selectivity

Resistive gas sensors with metal oxide layers are frequently used for monitoring environmental gases particularly toxic gases in air due to their high response and good long term stability. The cross sensitivities of the sensor towards different concentrations of H_2S, CO, H_2, and C_2H_2 were measured at 300°C (Fig. 7). The sensor evidently shows much less response to CO, H_2, and C_2H_2 than to H_2S indicating high selectivity for H_2S of the SnO_2 sensor at the lower concentration (10 ppm). The selectivity experiment for SnO_2 sensing film was carried out by monitoring changes in resistance upon exposure to several gases in both high (200 ppm, 500 ppm) and low concentration (10 ppm) ranges. The several environmental gases were also comparatively tested at the concentrations of 200 ppm for CO, and H_2S, 500 ppm for H_2 and 10 ppm for H_2S at the operating temperature of 300°C. The other environmental gases (CO, H_2, and C_2H_2) were tested at relatively high concentrations because their responses were negligible at the low concentration of 10 ppm. It can be clearly seen that the SnO_2 sensor is evidently higher selective towards H_2S through the lower concentration as it exhibits much higher resistance increase after interaction with H_2S gas molecules at the operating temperature of 300°C. On the other hand, there are much small decreases in the sensor resistance upon exposure to other interfering gases including CO, H_2 and C_2H_2.

Table 1. Summary of gas-sensing performances of pure SnO_2 materials prepared by various synthetic methods

Authors	Methods	Materials	Gas Conc.	Sensing performances		
				Response (*S*)	t_{res}	Selectivity
Sahm *et al.* [10]	FSP (nanopowders) Drop coating (sensors)	Pure SnO_2	NO_2 (10–5,000 ppb), CO (500–10,000 ppm), propanol (10–300 ppm)	NO_2; ~ 20 to 5,000 ppb at 220°C Propanal; ~300 to 150 ppm at 220°C	-	NO_2; *S* ~ 20 to 5,000 ppb
Mädler *et al.* [11]	FSP (nanopowders) Thermophoretic deposition (sensors)	0.2 wt%Pt/SnO_2	CO; 50 ppm	8 to 50 ppm at 350°C	-	-
Jin *et al.* [3].	DC magnetron sputtering (sensors)	Pure SnO_2 films, Ag-, Cu-, Pt-, Pd-doped SnO_2 films (1–16 nm)	H_2S; 1 ppm	Doping film = 16 nm Response to H_2S at 200°C, 5900; 1 ppm at 250°C, 590; 1 ppm	second	-
Gong *et al.* [4]	Sol-gel	Pure SnO_2 and Ag/SnO_2	H_2S; 1–25 ppm	> 120 to 10 ppm, 70°C, 9% R.h. ~ 90 to 5 ppm, 70°C, 9% R.h. ~ 55 to 2 ppm, 70°C, 9% R.h.	-	H_2S, *S* > 120 to 10 ppm, 70°C Other gases; *S* < 3 Cl_2 (10 ppm), HCl (10 ppm), HCN (10 ppm), SO_2 (9 ppm), C_6H_{14} (0.3%), CH_4 (2.2%), CO (50 ppm), C_3H_8 (0.44%), NO_2 (5 ppm)
Griessler *et al.* [5]	Spray pyrolysis process	Pure SnO_2 thin film (50 ppm)	H_2S (2.5 ppm) and SO_2 (50 ppm)	H_2S (2.5 ppm), 400°C, ~ 85% SO_2 (50 ppm), 300°C, ~ 40%	-	-
Das *et al.* [9]	Simultaneous precipitation technique (nanopowders) Screen printing (sensor)	Pure SnO_2 (40–50 nm) and 0.1–1 wt%V_2O_5/SnO_2 (14–17 nm)	SO_2 (5, 100 ppm)	Response of SO_2 (5 ppm) at 350°C of SnO_2 (~ 20%) and 0.15 wt%V_2O_5/SnO_2 (~ 45%) Response to 100 ppm at 350°C of SnO_2 (~ 35%) and 0.15 wt%V_2O_5/SnO_2 (~ 70%)	-	*S* < 30% CH_4 (100 ppm), CH_4H_{10} (100 ppm), CO (100 ppm)
Present work	FSP (nanopowders) Spin coating (sensors)	Pure SnO_2	SO_2; 20–500 ppm H_2S; 0.5–10 ppm	Response to 20–50 ppm of SO_2 ~3.8–6.8, 300°C Response to 0.5–10 ppm of H_2S ~1.4–8.4, 300°C	500 ppm of SO_2 10 s, 300°C 10 ppm of H_2S 3 s, 300°C	Other gases like CO (200 ppm); C_2H_2 (200 ppm), H_2 (500 ppm) *S* < 2

DOI:10.4186/ej.2012.16.3.123

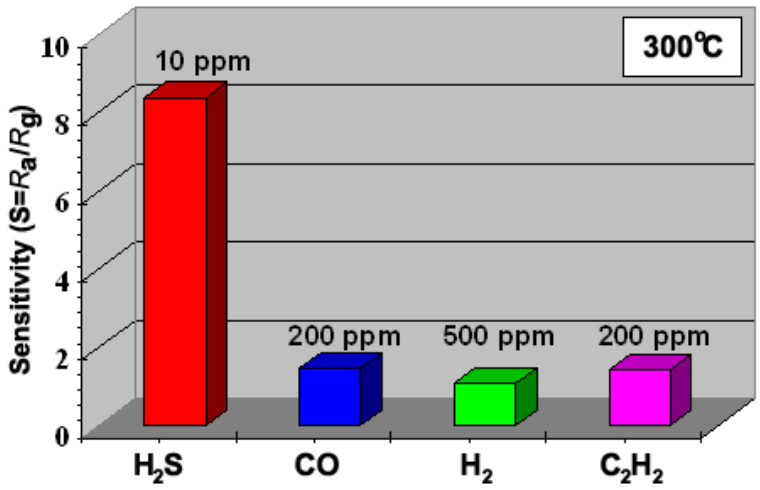

Fig. 7. The selectivity histogram of SnO_2 sensor for environmental monitoring including the H_2S, CO, H_2 and C_2H_2 at low concentration of 10 ppm for H_2S and high concentrations of 200 ppm and 500 ppm for CO, C_2H_2 and H_2, respectively, at the operating temperatures of 300°C.

3.4. Sensing Film Morphology

The cross-section, film thickness, and surface morphology of the SnO_2 sensing layer after annealing and sensing ranging from 200–350°C were observed using SEM analysis as shown in Fig. 8. It can be seen that the film thickness of sensing film is approximately 5 μm (side view), which benefits tremendously to gas-sensing properties. The SnO_2 sensing layer is crack-free and contains very high density nanoparticles. It was formed after annealing in air for binder removal at 400°C for 1h and repeated gas-sensing measurement ranging from 200–350°C. After annealing and sensing processes, a denser film layer was formed. The regularity in the film thickness stems from the uniformity of binder-powder mixing and spin coating process.

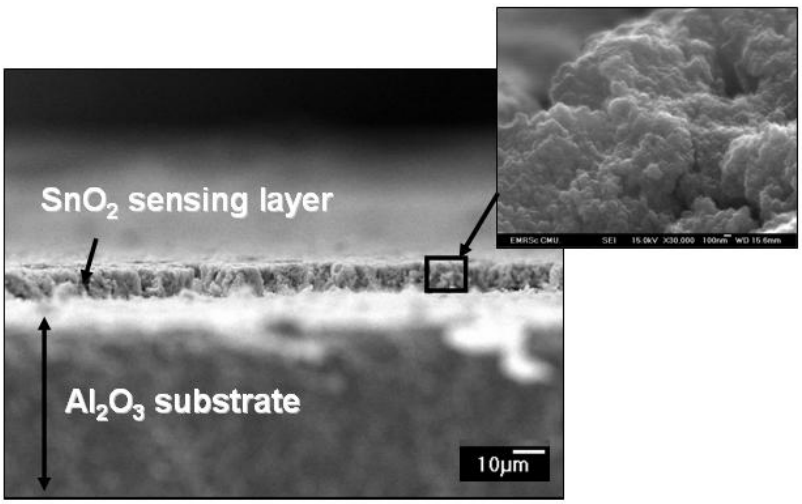

Fig. 8. SEM micrographs of SnO_2 sensing film spin-coated on an Al_2O_3 substrate with interdigitated Au electrodes after annealing at 400°C and gas-sensing measurement ranging from 200–350°C in dry air. The film thickness was approximately 5 μm.

4. Conclusions

In conclusion, the monitoring of suitable sensitive sensors for noxious gas in an industrials environment was fabricated by spin coating of flame-spray-made SnO_2 nanoparticles. The sizes and dimensional

structures (outer diameter of nanoparticles and 2D film thickness) played an important role in increasing the specific surface area of sensing layer. The nanoparticles were found to have a high specific surface area (SSA_{BET}: 141.6 m^2/g), which could significantly enhance surface ionization reaction from adsorption and desorption of oxygen and gas species. The continuous sensing film was achieved leading to the connectivity of nanoparticles' properties. The SnO_2 sensor was tested to H_2S and SO_2 with different concentration ranges. The SnO_2 sensor exhibited much higher response and selectivity to H_2S (to 10 ppm, S=8.4) against other gases at high concentration and operating temperature of 300°C. The response time was very fast (3s) to 10 ppm of H_2S gas. Therefore, the SnO_2 sensor was one of the most suitable candidates for the efficient detection of noxious H_2S gas at low ppm-level for leakage prevention from industrials environment.

Acknowledgements

The authors gratefully acknowledge the financial support from the Thailand Research Fund (TRF); the National Research University Project under the Office of the Higher Education Commission, Ministry of Education, the National Nanotechnology Center (NANOTEC), NSTDA, Ministry of Science and Technology, through its program of Center of Excellence Network, Thailand, the Materials Science Research Center, Department of Physics and Materials Science, Faculty of Science, Chiang Mai University, Thailand and National Electronics and Computer Technology Center (NECTEC), Pathumthani, Thailand.

References

[1] C. H. Liu, L. Zhang, and Y.-J. He, "Properties and mechanism study of Ag doped SnO_2 thin films as H_2S sensors," *Thin Solid Films*, vol. 304, pp. 13–15, Feb. 1997.

[2] R. S. Niranjan, K. R. Patil, S. R. Sainkar, and I. S. Mulla, "High H_2S-sensitive copper-doped tin oxide thin film," *Mater. Chem. Phys.*, vol. 80, pp. 250–256, Oct. 2003.

[3] C. Jin, T. Yamazaki, K. Ito, T. Kikuta, and N. Nakatani, "H_2S sensing property of porous SnO_2 sputtered films coated with various doping films," *Vacuum*, vol. 80, pp. 723–725, 2006.

[4] J. Gong, Q. Chen, M-R. Lian, N-C. Liu, R. G. Stevenson, and F. Adami, "Micromachined nanocrystalline silver doped SnO_2 H_2S sensor," *Sens. Actuators B: Chem.*, vol. 114, pp. 32–39, June 2006.

[5] C. Griessler, E. Brunet, T. Maier, S. Steinhauer, A. Köck, T. Jordi, F. Schrank, and M. Schrems, "Tin oxide nanosensors for highly sensitive toxic gas detection and their 3D system integration," *Microelec. Eng.*, vol. 88, pp. 1779–1781, Feb., 2011.

[6] C. M. Ghimbeu, M. Lumbreras, J. Schoonman, and M. Siadat, "Electrosprayed metal oxide semiconductor films for sensitive and selective detection of hydrogen sulfide," *Sensors*, vol. 9, pp. 9122–9132, Nov., 2009.

[7] C. M. Ghimbeu, M. Lumbreras, M. Siadat, R. C. van Landschoot, and J. Schoonman, "Electrostatic sprayed SnO_2 and Cu-doped SnO_2 films for H_2S detection," *Sens. Actuators B: Chem.*, vol. 133, pp. 694–698, Apr. 2008.

[8] J. Kaur, S. C. Roy, and M. C. Bhatnagar, "Highly sensitive SnO_2 thin film NO_2 gas sensor operating at low temperature," *Sens. Actuators B: Chem.*, vol. 123, pp. 1090–1095, 2007.

[9] S. Das, S. Chakraborty, O. Parkash, D. Kumar, S. Bandyopadhyay, S. K. Samudrala, A. Sen, and H. S. Maiti, "Vanadium doped tin dioxide as a novel sulfur dioxide sensor," *Talanta*, vol. 75, pp. 385–389, Nov. 2008.

[10] T Sahm, L. Mädler, A. Gurlo, N. Barsan, S. E. Pratsinis, and U. Weimar "Flame spray synthesis of tin dioxide nanoparticles for gas sensing*," Sens. Actuators B: Chem.*, vol. 98, pp. 148–153, 2004.

[11] L. Mädler, A. Roessler, S. E. Pratsinis, T. Sahm, A. Gurlo, N. Barsan, and U. Weimar, "Direct formation of highly porous gas-sensing films by in situ thermophoretic deposition of flame-made Pt/SnO_2 nanoparticles," *Sens. Actuators B: Chem.*, vol. 114, pp. 283–295, 2005.

[12] L. Mädler, T. Sahm, A. Gurlo, J.-D. Grunwaldt, N. Barsan, U. Weimar, and S. E. Pratsinis, "Sensing low concentrations of CO using flame-spray-made Pt/SnO_2 nanoparticles," *J. Nanopart. Res.*, vol. 8, pp. 783–796, 2006.

[13] C. Liewhiran and S. Phanichphant, "Influence of thickness on ethanol sensing characteristics of doctor-bladed thick film from flame-made ZnO nanoparticles," *Sensors*, vol. *7*, pp. 185–201, 2007.

[14] C Liewhiran and S. Phanichphant, "Improvement of flame-made nanoparticulate thick film morphology for ethanol sensing," *Sensors,* vol. 7, pp. 650–675, 2007.

[15] C. Liewhiran and S. Phanichphant, "Effects of palladium loading on the response of a thick film flame-made Zno gas sensor for detection of ethanol vapor," *Sensors*, vol. 7, pp. 1159–1184, 2007.
[16] C. Liewhiran and S. Phanichphant "Doctor-bladed thick films of flame-made Pd/ZnO nanoparticles for ethanol sensing," *Curr. Appl. Phys.*, vol. 8, pp. 336–339, 2008.
[17] C. Liewhiran, N. Tamaekong, A. Wisitsoraat, and S. Phanichphant, "H_2 sensing response of flame-spray-made Ru/SnO_2 thick films fabricated from spin-coated nanoparticles," *Sensors*, vol. 9, pp.8996–9010, 2009.
[18] S. E. Pratsinis, "Flame aerosol synthesis of ceramic powders," *Prog. Energ. Combust.*, vol. 24 pp. 197–219, 1998.
[19] L. Mädler, H. K. Kammler, R. Mueller, and S. E. Pratsinis, "Controlled synthesis of nanostructured particles by flame spray pyrolysis," *J. Aeros. Sci.,* vol. 33, pp. 369–389, 2002.
[20] R. Mueller, L. Mädler, and S. E. Pratsinis, "Nanoparticle synthesis at high production rates by flame spray pyrolysis," *Chem. Eng. Sci.*, vol. 58, pp. 1969–1976, 2003.